Applications of Microlocal Analysis in Compton Scattering Tomography and the Geodesic Ray Transform

Sean Holman
University of Manchester

BIRS Workshop:
Probing the Earth and the Universe with Microlocal Analysis

Based on joint work with Francois Monard, Plamen Stefanov and James Webber.

Outline

1. General comments about microlocal analysis in inverse problems.
2. Example: Compton scattering tomography.
3. Example: Geodesic ray transform.

Microlocal analysis (MA) in inverse problems

General formulation of linear inverse problem

$$\mathcal{A}[f] = d.$$

Some notation/terminology

- The wavefront set of f will be $WF(f)$.
- Elements of $WF(f)$ will be called singularities of f.
- $\mathcal{A}$ will be a Fourier integral operator (FIO) with canonical relation $\Lambda_{\mathcal{A}}$.

Microlocal analysis (MA) in inverse problems

General formulation of linear inverse problem

$$\mathcal{A}[f] = d.$$

MA inversion

If we have $WF(d)$, can we always find $WF(f)$?

- If the answer is yes, we say $\mathcal{A}$ is microlocally (MA) invertible.
- Microlocal invertibility corresponds with the ability to find the sharp edges, or high frequency features, of a given image from provided data.
- MA inversion is also related to stability. As a heuristic:

$$\text{MA inversion possible} \Leftrightarrow \text{Problem is mildly ill-posed.}$$

Microlocal inversion

Microlocal kernel

If

$$WF(\mathcal{A}[f]) = \emptyset$$

then we say that f is in the microlocal kernel, or μ-kernel, of $\mathcal{A}$.

- If $\mathcal{A}$ is an *FIO*, then $f \in C^\infty$ implies that f is in the μ-kernel of $\mathcal{A}$.
- Because of this we understand elements of the μ-kernel only modulo C^∞, and say that the μ-kernel is trivial when it contains only smooth functions.

Microlocal inversion

Microlocal kernel

If

$$WF(\mathcal{A}[f]) = \emptyset$$

then we say that f is in the microlocal kernel, or μ-kernel, of $\mathcal{A}$.

- The operator $\mathcal{A}$ may have an inverse, but still have non-trivial μ-kernel.
- Existence of a non-trivial μ-kernel contradicts the existence of any stability estimate in the form

$$\|f\|_{H^{s_1}} \leq C\|\mathcal{A}[f]\|_{H^{s_2}}$$

  for any Sobolov spaces H^{s_1} and H^{s_2}. In this case I say the problem is **severely** ill-posed).
- Elements of the μ-kernel will often correspond with artifacts.

MA in inverse problems reprise

Generic inverse problem

$$\mathcal{A}[f] = d.$$

Ideally $\mathcal{A}$ has elliptic symbol and $\Lambda_{\mathcal{A}}$ is a one-to-one map (i.e. a graph). Then we have MA inversion; the μ-kernel is trivial. However ...

Things that can go wrong...

1. There can be singularities of f that are not represented in $\Lambda_{\mathcal{A}}[f]$.These singularities are simply not measured in the data, and cannot be recovered.
2. $\Lambda_{\mathcal{A}}$ can be many-to-one. In this case the singularities of f may be able to cancel in $\mathcal{A}[f]$ creating a non-trivial μ-kernel.
3. $\Lambda_{\mathcal{A}}$ can be one-to-many so that a single singularity may create additional singularities in $WF(d)$ ...

The Normal Operator

To analyze the continuity or stability of an operator $\mathcal{A}$ we often consider the **normal operator**

$$\mathcal{N}_{\mathcal{A}} = \mathcal{A}^* \mathcal{A}$$

- $\mathcal{A}^*$ is the adjoint; for us with respect to the L^2 inner product.
- $\Lambda_{\mathcal{A}^*} = \Lambda_{\mathcal{A}}^{-1}$.

Adjoint is microlocal inversion

Because of the last point, when $\Lambda_{\mathcal{A}}$ is one-to-one $\mathcal{A}^*$ realises a microlocal inversion, and $\mathcal{N}_{\mathcal{A}}$ is a ΨDO.

- Stability estimates in inverse problems can be obtained by constructing a paramterix for $\mathcal{N}_{\mathcal{A}}$ when it is a ΨDO.
- In inverse problems $\mathcal{A}^*$ is often called “back-projection”.

Now let’s look at what happens when things go wrong!

Case 1 Example: Limited angle Radon transform.

Example: 2D Radon transform

$$R[f](s,\theta) = \int_{\omega\cdot x = s} f(x)\,\mathrm{d}H^1(x) \quad s \in \mathbb{R},\ \omega = (\cos(\theta), \sin(\theta)) \in \mathbb{S}^1$$

- If θ is restricted to $(0,\pi)$, then Λ_R is one-to-one with elliptic symbol (maybe a small problem at π ...).
- The limited angle case can be modelled by introducing a cut-off function χ in θ:

$$R_{lim}[f](s,\theta) = \chi(\theta) R[f](s,\theta).$$

- Literature: This example was studied by Frikel and Quinto.

Case 1 Example: Limited angle Radon transform.

Function f

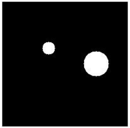

$R[f]$

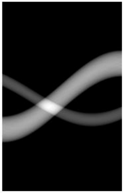

Restrict angle to $\theta \in [0, \pi/2]$

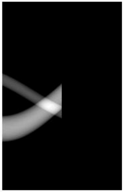

Reconstruction (FBP)

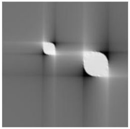

- Removed data correspond with singularities in blurred sections of dots.
- Sharp cut-off introduces singularities in data, which lead to artefacts.
- Streaking can be removed if χ is smooth, but blurring of edges cannot be fixed without other a priori information.

Example: Weighted geodesic ray transforms

Weighted geodesic ray transform

- (M, g) is an n dimensional Riemannian manifold with boundary.

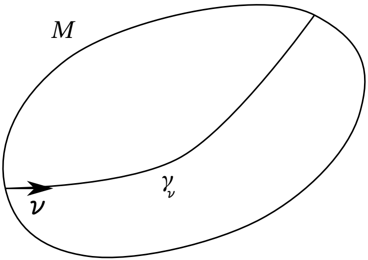

- Unit speed γ_ν geodesic starting at ν.
- $\kappa \in C^\infty(SM)$ a weight defined on the unit sphere bundle SM
- $f \mapsto \mathcal{X}[f](\nu) := \int f(\gamma_\nu(t))\, \kappa(\gamma_\nu(t), \dot\gamma_\nu(t))\, \mathrm{d}t.$

The weighted geodesic ray transform maps functions on M, to functions on the set of geodesics.

Case 2 Example: Unweighted geodesic ray transform with conjugate points

The geodesics are shown in red on the left.

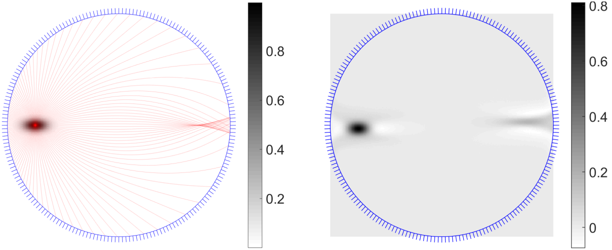

- This case was considered by Monard, Stefanov, and Uhlmann (2014).
- From a microlocal point of view, the transform of the left and right give the same information ... singularities cancel out.
- In this case the $\mathcal{N}_{\mathcal{X}}$ is the sum of a ΨDO and an FIO.

Cancellation of singularities, unweighted case

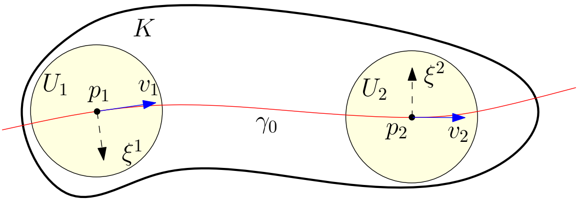

- p_1 and p_2 conjugate along geodesic tangent to v_1 and v_2.
- Then ξ_1 and ξ_2 map to the same point, say ω, under $\Lambda_{\mathcal{X}}$.
- Let X_1 and X_2 be microlocal representations of $\mathcal{X}$ in conic neighborhoods V_1 and V_2 of ξ_1 and ξ_2 respectively.

Cancellation of singularities, unweighted case

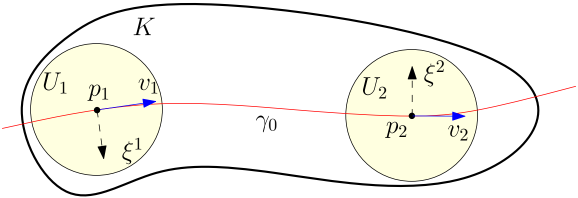

- If $WF(f) \subset V_1 \cup V_2$ we can write

$$f = f_1 + f_2$$

  where $WF(f_1) \subset V_1$ and $WF(f_2) \subset V_2$.
- Then reconstruction of $WF(f)$ is equivalent to microlocally inverting a system

$$X_1 f_1 + X_2 f_2 \approx \mathcal{X} f.$$

- Roughly speaking this is one equation for two unknowns which cannot be solved uniquely.

Cancellation of singularities, unweighted case

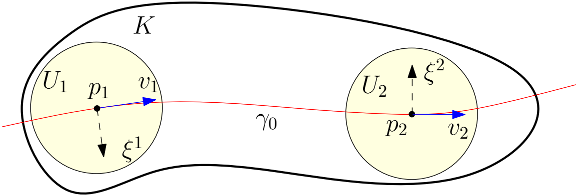

- Indeed, since X_1 (resp. X_2) is microlocally elliptic, a parametrix X_1^{-1} (resp X_2^{-1}) can be constructed.
- Thus for example

$$f_1 + X_2^{-1} X_1 f_1 \in \mu\text{-kernel}(\mathcal{X}).$$

- Note this argument could be used in any case for which $\Lambda_{\mathcal{A}}$ is many-to-one with elliptic symbol, showing cancellation of singularities can always occur in such cases.

Cancellation of singularities, unweighted case

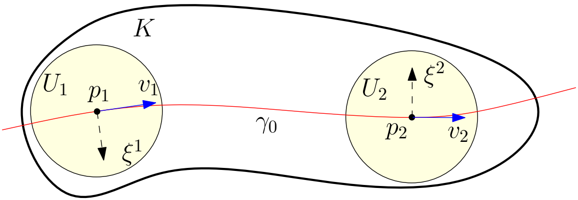

- In the weighted case, integration along the same geodesic in the opposite direction may give different information.
- Roughly speaking, because of this we get two equations, one for each direction, for the two unkowns f_1 and f_2.
- Because of this MA inversion may be possible for weighted transforms, although not when there are three points conjugate to one another along one geodesic.

Operators F_{ij}

We define

$$F_{21} = X_2^{-1} X_1, \quad F_{12} = X_1^{-1} X_2.$$

- These are FIOs with canonical relations mapping between V_1 to V_2.
- With this notation we have (in the unweighted case)

$$f_1 + F_{21} f_1, \quad f_2 + F_{12} f_2 \in \mu\text{-kernel}(\mathcal{X}).$$

- The operators

$$F_{12}^* F_{12}, \quad F_{12} F_{12}^*, \quad F_{21}^* F_{21}, \quad F_{21} F_{21}^*$$

  are order zero pseudodifferential operators.

Operators F_{ij}

Symbols, unweighted case

We have the following formulae for the principal symbols

$$\sigma_p\left(F_{12}^* F_{12}\right)(x,\xi) = \sigma_p\left(F_{12} F_{12}^*\right)(x,\xi) = |D_t J(t_0)|/|D_t J(0)|,$$
$$\sigma_p\left(F_{21}^* F_{21}\right)(x,\xi) = \sigma_p\left(F_{21} F_{21}^*\right)(x,\xi) = |D_t J(0)|/|D_t J(t_0)|.$$

- $J(t)$ is a Jacobi field vanishing at $p_1 = J(0)$ and $p_2 = J(t_0)$, D_t is the covariant derivative.

- The relative size of the Jacobi fields is related to the relative size of the artifact appearing in a Landweber reconstruction.

Landweber reconstruction

Expected Landweber reconstruction

Landweber iteration

$$f_n = f_{n-1} - \frac{1}{A}\mathcal{X}^*\frac{1}{\tau}(\mathcal{X} f_{n-1} - d) \quad \text{(Landweber)}$$

If $f = f_1$ is only singular in V_1, then we expect the Landweber iteration will converge to

$$\left[f_1 - (\mathrm{Id} + F_{21}^* F_{21})^{-1} f_1)\right] + \left[F_{21}(\mathrm{Id} + F_{21}^* F_{21})^{-1} f_1\right]$$

- This is the minimal $f \in L^2$ such that $\mathcal{X} f \approx d$ that is orthogonal to the μ-kernel($\mathcal{X}$) in a certain sense.
- The relative size of the derivatives of the vanishing Jacobi fields at the two conjugate points can give more precise information on the size of the artifact.

Landweber reconstruction

Expected Landweber reconstruction

Landweber iteration

$$f_n = f_{n-1} - \frac{1}{A}\mathcal{X}^* \frac{1}{\tau}(\mathcal{X} f_{n-1} - d) \quad \text{(Landweber)}$$

If $f = f_1$ is only singular in V_1, then we expect the Landweber iteration will converge to

$$\left[f_1 - (\mathrm{Id} + F_{21}^* F_{21})^{-1} f_1)\right] + \left[F_{21}(\mathrm{Id} + F_{21}^* F_{21})^{-1} f_1\right]$$

- If the size of the derivatives of the Jacobi fields is the same, then this is

$$\approx \frac{1}{2} f_1 + \frac{1}{2} F_{21} f_1.$$

Example

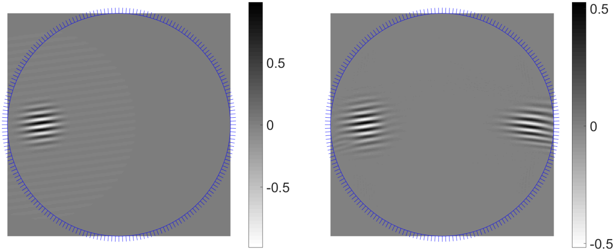

- Left is phantom, right is reconstruction.
- The L^2 size of the artifact is the same as the L^2 size of the correct reconstruction.

Weighted Examples

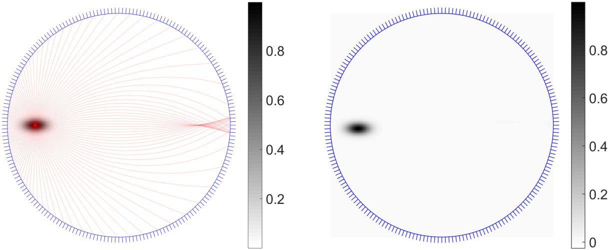

- This is the same metric as previous example, the difference is that a positive attenuation is added.
- Reconstruction method is the same.
- The weight removes the artifacts in the reconstruction.

Weighted Examples

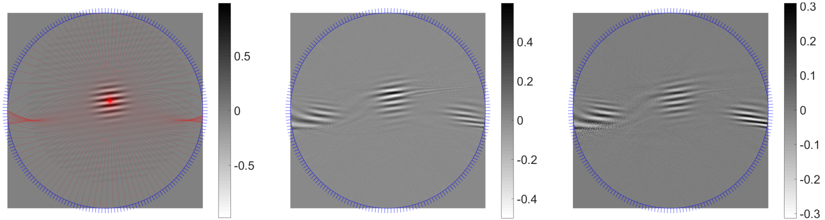

- In this example there is a point with two conjugate points along a single geodesic.
- The middle reconstruction is with no weight, the right is with a weight.

Contrast with 3D case

The 3D case is different. Recall the 2D example with three conjugate points along a given geodesic from before.

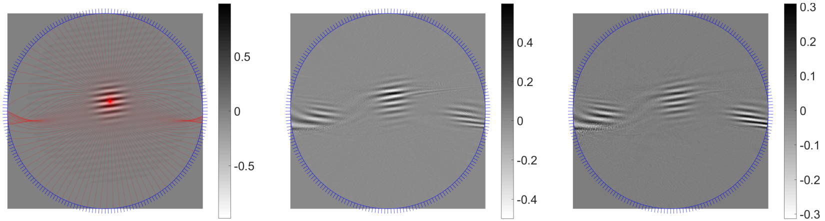

We create a similar 3D example by rotating this metric around its axis of symmetry.

Constrast with 3D case

Same type problem in 3D (unweighted).

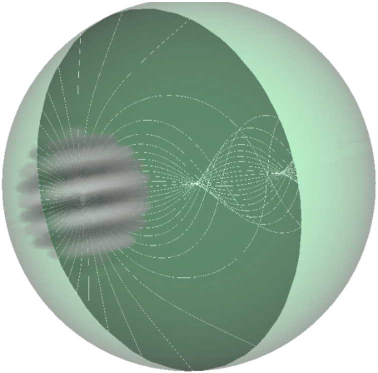

- Reconstruction is stable in this case because of geodesics passing orthogonally to the “gutter” which do not have conjugate points.

Case 3 Example: Compton scattering tomography

Background

- Compton scattering describes an inelastic collision between a photon and an electron:

$$E_s = \frac{E_\lambda}{1 + (E_\lambda / E_0)(1 - \cos\omega)}$$

  - E_s is the energy of the scattered photon.
  - E_λ is the energy of the incident photon.
  - E_0 is the electron rest energy.
  - ω is scattering angle.
- Loss of energy corresponds with scattering angle ω.

Case 3 Example: Compton scattering tomography

Set-up for a fixed source

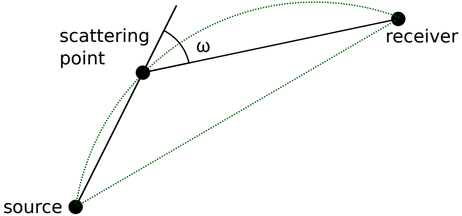

- For fixed E_s and E_λ, the measurement will be an integral of electron density over the surface of revolution of a circular arc connecting the source and receiver.
- We consider the case when $\omega < \pi/2$. Then the surface is called a *spindle torus*.

A bit of literature

- There is a survey on Compton scattering tomography by Truong and Nguyen [2012].
- In two dimensions we have a transform involving integrals over circular arcs. In this case there are analytic inversion formulae (Palamodov [2011]).
- More recently there has been quite a bit of work on “cone transforms” of various types arising from Compton scattering. Analytic reconstruction formulae have been found in some cases. (e.g. see Ambartsoumian [2012,2013], Haltmeier [2014], Kuchment and Terzioglu [2016], ...)

Our scanning geometry

We considered a specific geometry proposed for three dimensional Compton scattering tomography.

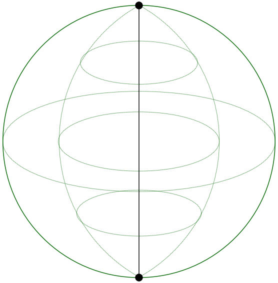

- Source and receiver are at antipodal points on the unit sphere.
- Antipodal points are freely chosen on the sphere.

Spindle transform

Definition: Spindle transform

For $0 < \epsilon_1 < \epsilon_2 < 1$, let $B_{\epsilon_1,\epsilon_2} \subset \mathbb{R}^3$ be defined by

$$B_{\epsilon_1,\epsilon_2} = \{x \in \mathbb{R}^3 \ : \ \epsilon_1 < |x| < \epsilon_2\}.$$

Then the *spindle transform* $\mathcal{S} : C_0^\infty(B_{\epsilon_1,\epsilon_2}) \to C^\infty((0,1)_r \times \mathbb{S}^2_\theta)$ maps f to its integral over the spindle described by $(r,\theta) \in (0,1)_r \times \mathbb{S}^2_\theta$.

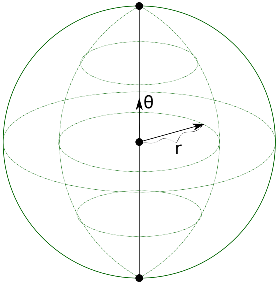

Results on the spindle transform

- The spindle transform is not injective because spindles with axis through the origin are invariant under reflection through the origin.
- Because of this, if $f \in C_0^\infty(B_{\epsilon_1,\epsilon_2})$ and

$$g(x) = f(-x),$$

then

$$\mathcal{S}f = \mathcal{S}g.$$

- The spindle transform was shown to be injective restricted to a functions supported in a half-space by Webber and Lionheart [2018].

Spindle torus

Implicit equation of spindle torus

$$(r + |\theta \times x|)^2 + (x \cdot \theta)^2 = 1 + r^2.$$

- x is a point on the spindle torus.
- r is tube centre offset.
- $\theta \in \mathbb{S}^2$ gives the axis of rotation for the spindle.

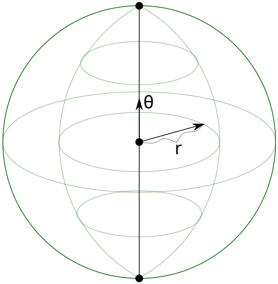

Spindle transform

Spindle transform: formula

If we set

$$h(s,x,\theta) = \frac{4|x\times\theta|^2}{(1-|x|^2)^2} - s,$$

then the spindle transform is given by

$$\mathcal{S}f(1/s^{1/2},\theta) = \int_{B^3_{\epsilon_1,\epsilon_2}} \frac{\delta\left(\frac{4|x\times\theta|^2}{(1-|x|^2)^2} - s\right)}{|\nabla_x h(s,x,\theta)|} f(x)\mathrm{d}x.$$

- From this we can see that the spindle transform is a Fourier Integral Operator (FIO).
- Microlocal analysis could proceed from this formula, but we take a slightly different approach ...

Transformation from spindles to cylinders

The spindle transform is related to a weighted cylinder transform.

Transformation

Set

$$v(x) = \left(\sqrt{1 + \frac{1}{|x|^2}} - \frac{1}{|x|}\right) \cdot \frac{x}{|x|}, \quad \alpha_i = 2\epsilon_i/(1 - \epsilon_i^2)$$

and

$$\tilde{f}(x) = |\det(J_v)|\, f\,(v(x))$$

(J_v the Jacobian of $x \mapsto v(x)$). Then

$$\mathcal{S}f(1/s^{1/2}, \theta) = \int_{B^3_{\alpha_1,\alpha_2}} \frac{\delta\left(|x|^2 - (x\cdot\theta)^2 - s\right)}{|\nabla_v h(s, v(x), \theta)|} \tilde{f}(x)\, \mathrm{d}x := \mathcal{C}\tilde{f}(s, \theta)$$

Cylinder transform

Cylinder transform definition

$$\mathcal{C}\tilde{f}(s,\theta) = \int_{B^3_{\alpha_1,\alpha_2}} \frac{\delta\left(|x|^2 - (x\cdot\theta)^2 - s\right)}{|\nabla_v h(s, v(x), \theta)|} \tilde{f}(x)\,\mathrm{d}x$$

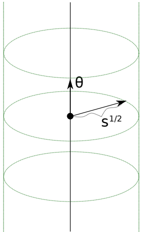

- Note that $\mathcal{C}\tilde{f}(s,\theta)$ is a weighted integral of $\tilde{f}$ over the cylinder with axis through the origin given by θ, and radius $s^{1/2}$.

Cylinder transform

Theorem: Cylinder transform as an FIO

The cylinder transform $\mathcal{C}$ is a Fourier integral operator order -1 with canonical relation

$$\begin{aligned}\Lambda_{\mathcal{C}} = &\Big\{\Big((s,\alpha,\beta),(\sigma, 2\sigma(x\cdot\theta_\alpha)(x\cdot\theta), 2\sigma(x\cdot\theta_\beta)(x\cdot\theta)); x,\\ &2\sigma(x-(x\cdot\theta)\theta)\Big) \ : \ x \in B^3_{\alpha_1,\alpha_2},\ s\in(0,\infty), \sigma\in\mathbb{R}\backslash 0, \theta\in S^2,\\ &|x|^2-(x\cdot\theta)^2 - s = 0\Big\},\end{aligned}$$

where $(\alpha,\beta)\in\mathbb{R}^2$ provide a local parameterization of $\theta\in\mathbb{S}^2$, $\theta_\alpha = \partial_\alpha\theta$ and $\theta_\beta = \partial_\beta\theta$.

- Note that $\mathcal{C}$ suffers from the same problem with symmetry as $\mathcal{S}$, and $C_{\mathcal{C}}$ is two-to-one at most points because of this.
- Note there is also an issue at $(x,\xi = 2\sigma x)$ when $x\cdot\theta = 0$. At such points $C_{\mathcal{C}}$ is one-to-many.

A return to general theory: The Normal Operator

Recall the normal operator

$$\mathcal{N}_{\mathcal{C}} = \mathcal{C}^*\mathcal{C}.$$

Theorem: $\mathcal{N}_{\mathcal{C}}$ as a paired Lagrangian operator

- The left and right projections of $\Lambda_{\mathcal{C}}$ have blowdown singularities of order 1 along a codimension 1 submanifold Σ.
- We have $\mathcal{C}^*\mathcal{C} \in I^{-2,0}(\Delta, \Lambda) + I^{-2,0}(\widetilde{\Delta}, \Lambda)$.
- Δ is the diagonal in $T^*B^3_{\alpha_1,\alpha_2} \times T^*B^3_{\alpha_1,\alpha_2}$
- $\widetilde{\Delta} = \{(-x, -\xi; x, \xi) \ : \ (x, \xi) \in T^*B^3_{\alpha_1,\alpha_2}\}$
- Λ is the flowout of $\pi_R(\Sigma)$.

The Flowout

- The singular manifold $\Sigma \subset \Lambda_{\mathcal{C}}$ is

$$\Sigma = \{x \cdot \theta = 0\} \cap \Lambda_{\mathcal{C}}.$$

- The flowout Λ is

$$\Lambda = \{(x, \xi; \mathcal{O}(x, \xi)) \ : \ x \in B^3_{\alpha_1, \alpha_2}, \\ \xi \in \mathbb{R}^3 \setminus 0, \quad x \times \xi = 0, \quad \mathcal{O} \in \Delta(SO_3 \times SO_3)\}.$$

- **Consequence:** If we apply backprojection ($\mathcal{C}^*$) to reconstruct, and there are radially oriented singularities, then we expect artefacts will appear on the sphere with that singularity in its normal bundle.
- Because the transformation between cylinder and spindle transforms is radial, the same is true for the spindle transform.

Numerical Example of $\mathcal{N}_\mathcal{S}$

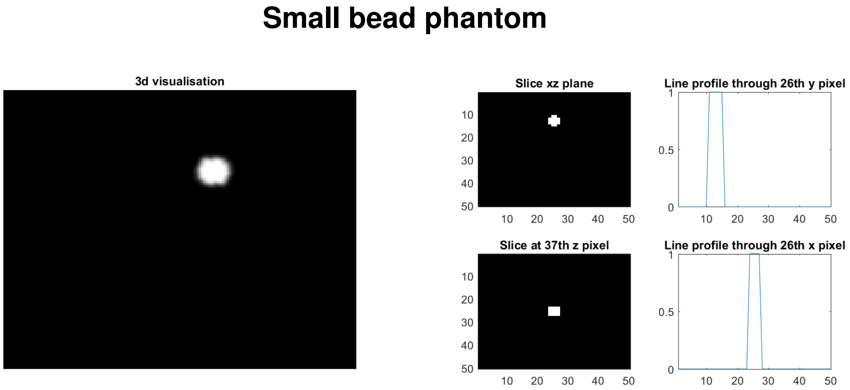

Numerical Example of $\mathcal{N}_{\mathcal{S}}$

Backprojection reconstruction ($\mathcal{N}_{\mathcal{S}}$)

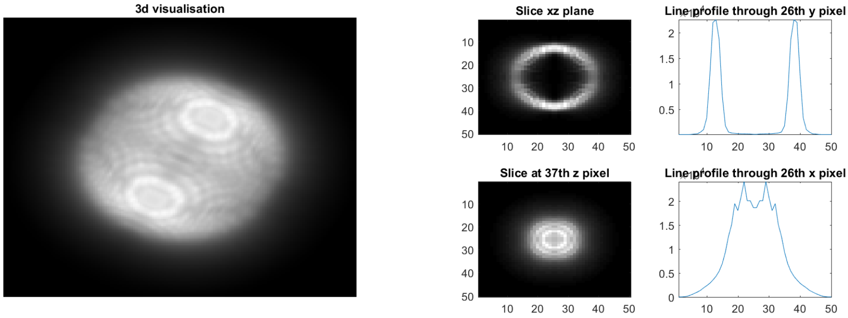

Reducing Artefacts

Problem causing artefacts

- Since $\mathcal{N}_{\mathcal{C}} \in I^{-2,0}(\Delta, \Lambda) + I^{-2,0}(\widetilde{\Delta}, \Lambda)$, the artifacts caused by Λ have the same strength as the image (and its reflection through the origin).
- Same is true for $\mathcal{N}_{\mathcal{S}}$.

Proposed solution

- Felea, Gaburro, and Nolan [2013] suggested including a pseudodifferential filter Q

$$\mathcal{N}_{\mathcal{S}} \mapsto \mathcal{N}_{\mathcal{S}}^{Q} := \mathcal{S}^{*} Q \mathcal{S}.$$

  to reduce artefacts in a similar case.
- If $Q \in \Psi^{0}$ is chosen to vanish to appropriate order on the left projection of Σ, then the strength of the artefacts will be reduced.

Reducing Artefacts

Pseudodifferential filter

In our case we use

$$Q = -\Delta_{S^2} \left(I - \Delta_{S^2} \right)^{-1}$$

- Here $\Delta_{\mathbb{S}^2}$ is the spherical Laplacian.
- In practice, we use spherical harmonics to apply Q.
- We call this reconstruction filtered backprojection

Numerical Example of Filtered Backprojection

Filtered backprojection reconstruction ($\mathcal{N}_{\mathcal{S}}^{Q}$)

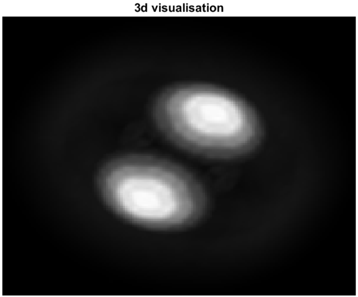

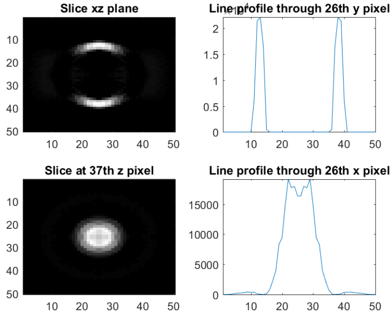

Practical Considerations

Arguably unfortunate truth of linear inverse problems

Iterative solvers available from numerical linear algebra work very well.

- These can largely be blind to the mathematics of particular applications except in how they construct the forward model.
- Also see Francois Monard's talk from Tuesday with MCMC methods, which applies also to nonlinear problems.

How can microlocal analysis inform practical applications?

- There is no replacement for proving identifiability, or proofs of stability.
- Stable reconstruction of singularities is still relevant even using iterative solvers.
- Other things as well ... .

Numerical Example: Radial Phantom

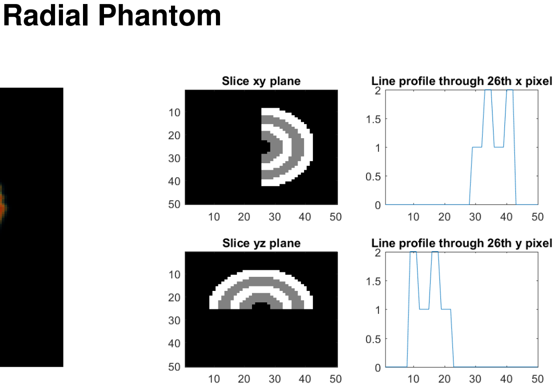

Numerical Example: Radial Phantom

CGLS reconstruction, 1% additive Gaussian noise, Tikhonov regularisation

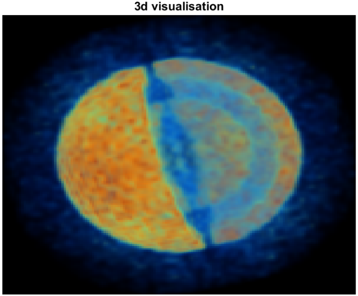

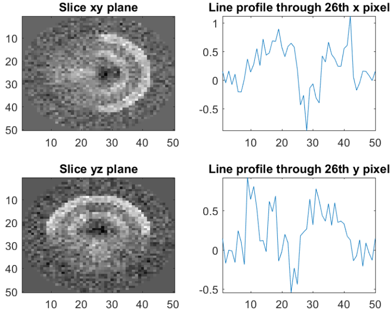

Numerical Example: Plane Phantom

Double decker sandwich phantom

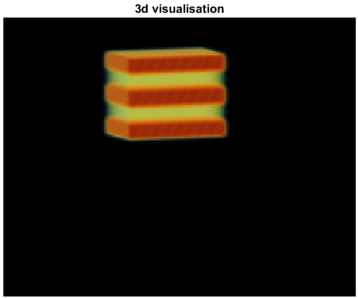

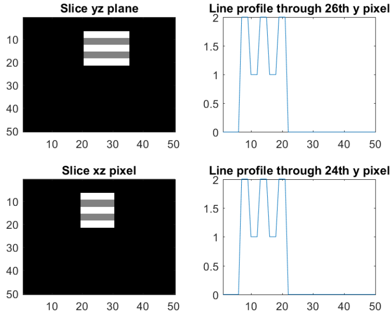

Numerical Example: Plane Phantom

CGLS reconstruction, 1% additive Gaussian noise

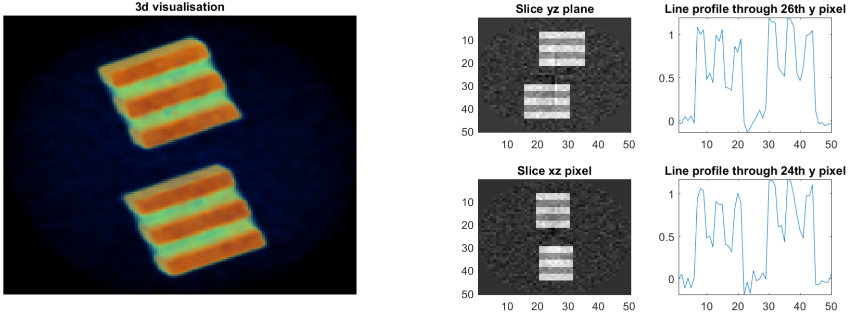

- Note layers in sandwich phantom are not radially oriented, and we have better reconstruction.

Conclusion

Thank you for your attention!